Sensors & Transducers, Vol. 267, Issue 4, December 2024, pp. 9-19

Sensors & Transducers
Published by IFSA Publishing, S. L., 2024
http://www.sensorsportal.com

Trial of Gait Analysis Using a Bilateral Gait Measurement System with Detailed Toe-tip Measurements

[1, *] Eiichi OHKUBO, [1] Yasutaka UCHIDA, [2] Tomoko FUNAYAMA and [3] Yoshiaki KOGURE

[1] Department of Life and Science, Teikyo University of Science, 2-2-1 Senju sakuragi, Adachi-ku Tokyo,125-0045, Japan
[2] Department of Occupational therapy, Teikyo University of Science, 2525, Yatsusawa, Uenoharashi, Yamanashi, 409-0193, Japan
[3] Professor Emeritus Teikyo University of Science, 2-2-1 Senju sakuragi, Adachi-ku Tokyo, 125-0045, Japan
[1] Tel.: +81369101010, fax: +81369103800
[*] E-mail:ohkubo@ntu.ac.jp

Received: 29 May 2024 / Revised: 3 December 2024 / Accepted: 17 December 2024
Published: 30 December 2024

Abstract: A prototype insole sensor capable of measuring the gaits of both feet was developed. Feature analysis was performed using data acquired from simultaneous measurements of both feet. In addition, a dataset of peak values and rates of change was created from the acquired data and its application in machine learning was investigated. The results of the analysis using random forests showed that the rate of change was better at detecting detailed movements at the measurement points. The significance of the data obtained from the toes was confirmed. Therefore, we conducted an additional study using an insole sensor with more toe measurement points. Analysis of the rate of change showed the possibility of classification using toe-tip data. Therefore, random forest and principal component analyses were used.

In this study, we demonstrated the usefulness of insoles for recording detailed individualized toe data. By accumulating and analyzing the data, we demonstrated the possibility of obtaining a guideline for the measurement location according to the subject's symptoms.

Keywords: Pressure sensors, Insole, Health condition change, Arduino, Bluetooth, Classification.

1. Introduction

With the advent of the super-aging society, the importance of preventive technologies in nursing and medical care has increased. In Japan, efforts to promote prevention before serious diseases occur, such as screening for metabolic syndrome, are being actively implemented to control rising medical costs [1]. Walking is fundamental to maintaining good health. As an essential activity in daily living, walking has been the focus of research aimed at linking its assessment to activities of daily living [2]. Gait analysis is being studied as a noninvasive method for evaluation individuals [3]. It is used not only for gait training in rehabilitation, but also for treatment evaluation, for example in Parkinson's disease [4, 5]. Traditionally, video analysis based on videography has been widely used for gait analysis. Advances in sensor technology have led to the use of 3D motion analysis systems [6] and mat-type pressure-sensitive sensors [7]. However, these methods are expensive and require large installation spaces. The insole sensor provides a simple measurement method. The position can be sensed by placing the insole sensor inside the

shoe. There are also research studies exploring the use of machine learning to estimate data from insole sensors [8]. In Japan, insole sensors that are inexpensive and easy to use are primarily designed for sports training, such as running and golf, rather than for rehabilitation purposes [9]. Some commercially available insole sensors are sized by cutting the entire insole at the same ratio for fine adjustments, while others are adjusted by cutting only the toe portion [10]. However, achieving uniform adjustments has proven challenging, with the proportions varying between the toe and heel sides.

Although the heel tends to be considered important because of the large amount of weight placed on it, we considered data other than the heel to be important parameters in the detection of gait disorders.

Therefore, we developed a prototype insole sensor that can perform measurements using an inexpensive general-purpose sensor and investigated the measurement points. We found that there were variations in the intensity of the measurement data other than at the heel, depending on the sensor position, confirming the importance of the sensor measurement point [11, 12].

Our previous system could not simultaneously measure both feet at the same time. We improved the system so that both feet could be measured simultaneously. Using the measurement data of both feet, we investigated the possibility of determining the sensor positions based on the characteristics of the subject's gait, symptoms, and treatment policy. Using the acquired data, we studied an analytical method for classifying the gait state using machine learning and presented the results at the recent SEIA 2024 conference [13].

This study describes the results of a trial run using an improved insole sensor capable of measuring toe conditions, addressing a new problem identified during the conference presentation.

The research was approved by the Ethics Committee of Teikyo University of Science.

2. Experience

2.1. Improvements to the Bilateral Gait Measurement System

An insole sensor that enables gait measurement of both feet is shown in Fig. 1. Four measurement locations were set up: toe, heel, outer, and inner.

The toe, inner, and outer sensors were placed 15 mm, 70 mm, and 80 mm from the toe, respectively. The heel sensor was placed 25 mm from the edge of the heel. The same insole sensors were used for the subjects measured in this study because their shoe sizes were 27 cm and 25 cm. An Arduino nano (hereinafter Arduino) was used as the microcomputer for control, and an FSR402 from Interlink electronics was used as the sensor device [14]. The transmitted data was sent using a recording Windows PC (hereafter PC) running a data recording program.

A voltage of 5 V was applied to the pressure sensor to convert the resistance change of the sensor into a voltage change. The voltage converted signal was input to the analog port of the Arduino. Since the analog port is a 10-bit conversion, the input value was decomposed into 1024 steps. The decomposed data is converted to the maximum value of 256 by quartering it to match the data acquired in the past.

Four sensors are measured in turn, and after the data from all the sensors are acquired, the data from the four sensors are sent to the computer as one data block with delimiters to improve the processing speed.

The data sampling interval is estimated to be about 50 milliseconds. The sampling frequency is estimated to be 20 Hz from the sampling interval.

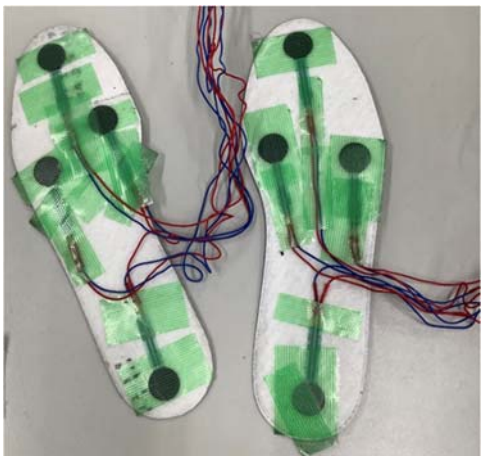

Fig. 1. Prototype insole sensor (bottom surface).

The system configuration is shown in Fig. 2.

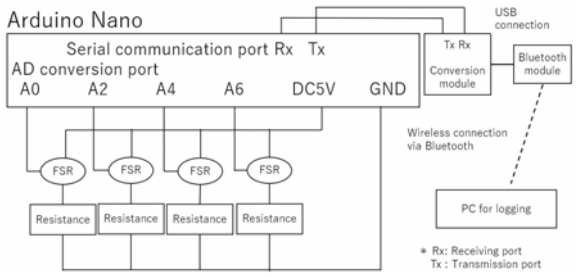

Fig. 2. System configuration.

A Bluetooth converter module acquires serial signals from the Arduino, which is placed on a 72 mm × 42 mm board with a 6F22 9 V battery. System components are sized to fit inside an adult shoe. The data acquisition interval of the PC is estimated to be about 0.1 sec maximum for one side based on the processing time of the Arduino and the delay caused by Bluetooth; data is recorded when the PC receives data from both sides. The devices on both

sides are not synchronized and send data to the PC independently.

The data received from the Arduino was recorded and stored in a Comma Separated Value (CSV) format file on the PC using a conversion program with processing. The elapsed time measured from the time of program operation on the PC was recorded in milliseconds, and the data was processed. The signals sent from the Arduino were recorded as one record in the CSV file as one set of data from both sides. An example of the data in the CSV file is shown in Table 1.

Table 1. Examples of recorded data.

time(s)	R toe	R out	R in	R heel	L toe	L out	L in	L heel	raw_R	raw_L
2.098	0	0	0	0	8	74	135	8	0 0 0 0	8 74 135 8
2.207	0	30	54	69	0	19	85	80	0 30 54 69	0 19 85 80
2.251	0	30	55	71	0	19	86	81	0 30 55 71	0 19 86 81
2.302	0	30	55	72	0	20	86	83	0 30 55 72	0 20 86 83
2.367	0	30	55	72	0	19	86	82	0 30 55 72	0 19 86 82

2.2. Improvements to the System with More Toe Measurement Points

To further analyze the toe data, we modified the insole sensors to include an additional toe measurement point and conducted additional experiments. The system configuration was modified to include two additional toe measurement points. A diagram of the modified system configuration is shown in Fig. 3.

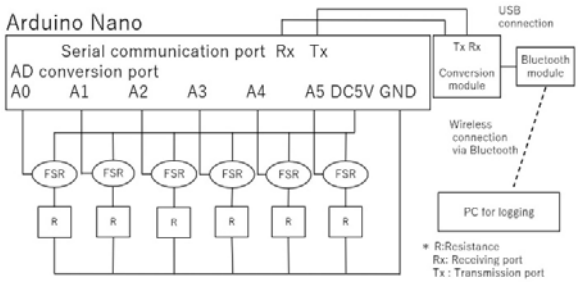

Fig. 3. System configuration after modification.

The Arduino used in this system comprised eight AD converters. As the number of measurement points increased to six, the port layout was changed to use six ports from A0 to A5. Because the assignment of the AD converters on the Arduino changed, the recording program running on the PC was also modified to correspond to the port assignment change. The circuit configuration, such as the sensor drive voltage, did not change. To avoid port-assignment errors when modifying the program, the elements in the raw data file were arranged in the same manner as in the AD conversion ports. An example of a modified data file is presented in Table 2.

Fig. 4 shows an enlarged view of the toe portion of the prototype insole. The distance from the toe to the center of the sensor was set at 10, 30, and 50 mm, with the 10 mm point representing the top of the toe and the 50 mm point representing the bottom of the toe. This configuration ensured that the pressure sensitive portions of the sensors did not overlap. If the same FSR402 was used, the flexible cable that received signals from the sensor and the sensor would overlap, and the pressure would not be applied correctly. Therefore, the FSR402 Shorttail, a model with the same sensing part but a shorter flexible cable, was used at the two additional locations.

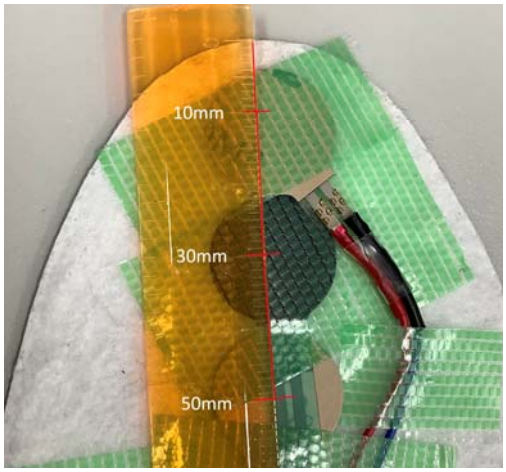

Fig. 4. Toe part improved on FSR402 (enlarged).

Table 2. Example of raw data file after modification.

time(s)	R toe	R out	R in	R heel	R toe top	R toe bottc	L toe	L out	L in	L heel	L toe top	L toe bottc	raw_R	raw_L
0.831	3	26	90	140	0	9	0	0	25	2	0	0	3 26 90 14	0 0 25 2 0 (
0.95	0	26	92	143	0	8	0	29	1	0	0	64	0 26 92 14	0 29 1 0 0 (
1.027	0	21	87	142	0	6	0	29	6	0	0	67	0 21 87 14	0 29 6 0 0 (
1.09	0	24	89	139	0	6	0	39	11	0	0	75	0 24 89 13	0 39 11 0 0
1.167	0	25	95	120	0	10	0	47	18	0	0	79	0 25 95 12	0 47 18 0 0

3. Results

3.1. Results of Bilateral Gait Measurements

Results of the experiment using data from healthy subjects are shown. A graph generated from the raw data is shown in Fig. 5. The transition of the acquired data waveforms indicated the shift in the load on both feet.

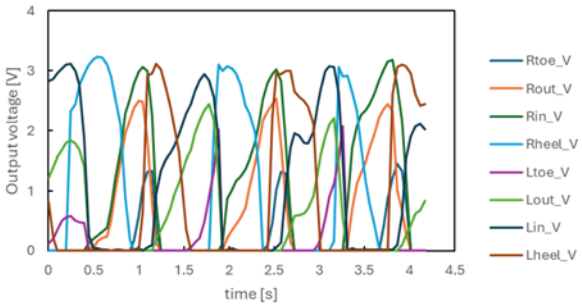

Fig. 5. Example of both feet (Right, Left) gait graph.

Gait feature extraction was performed to analyze the obtained data. Data were compared between normal walking and walking with a supporter attached to the subject's right knee to simulate a gait disorder. The data obtained were smoothed for feature extraction. Examples of the data from the right lateral sensor of the right foot, from which large features were obtained, are shown in Figs. 6 and 7. The vertical axis represents the standardized rate of change, and the horizontal axis represents the standardized sensor output voltage. The plotted data were cleansed, with the mean of the acquired data set to 0 and the standard deviation set to 1. Fig. 6 illustrates the feature extraction data in the normal state, with the center magnified.

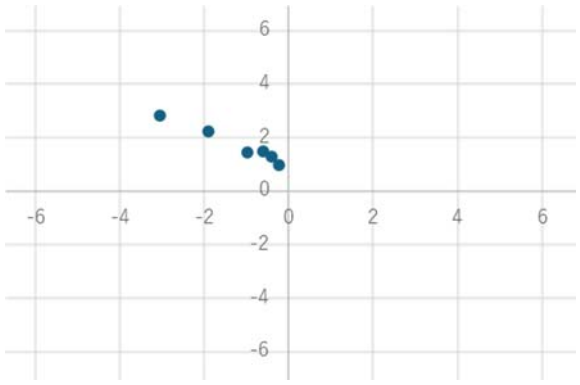

Fig. 6. Feature extraction (normal state).

Fig. 7 illustrates the feature extraction data in the right knee restriction state, with the center magnified.

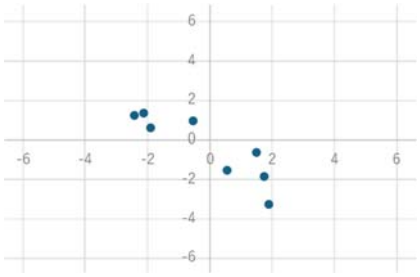

Fig. 7. Feature extraction (right knee restricted).

A comparison of Fig**.** 6 and 7 revealed that the set of plots tended to be divided between the normal and restricted states.

3.2. Increased Toe Measurement Results

As described in Section 3.2 a portion of Subject B's normal gait measurement data was clipped to generate a graph of the time variation of the input values to the AD converter. The results of all sensors on the right side are shown in Fig. 8; the results of the three sensor locations on the right toe are shown in Fig. 9; the results of all sensors on the left side are shown in Fig. 10; the results of three sensor locations on the left toe are shown in Fig. 11; the results of all sensors on both sides are shown in Fig. 12; the results of the three sensor locations on both toes are shown in Fig. 13.

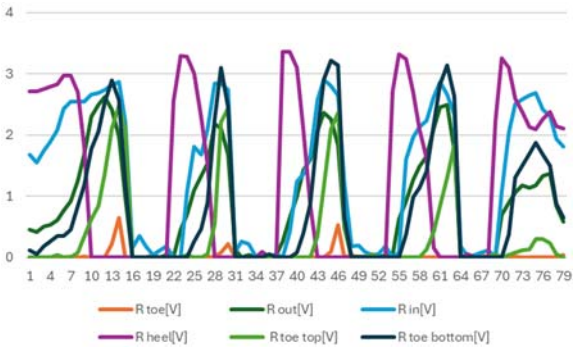

Fig. 8. Right side measurement data after modification.

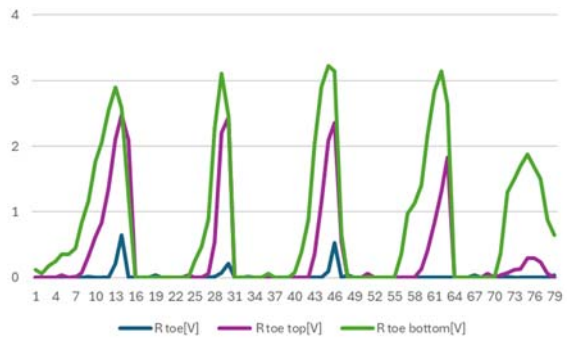

Fig. 9. Right side measurement data after modification (only 3 toe locations).

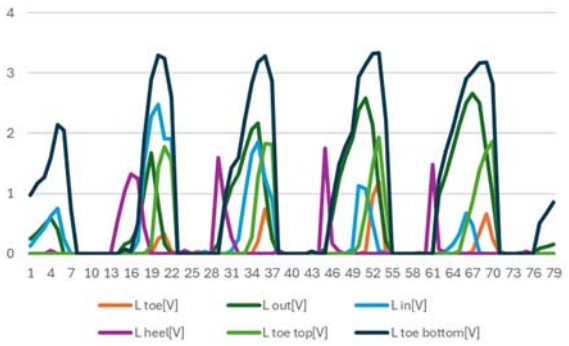

Fig. 10. Left side measurement data after modification.

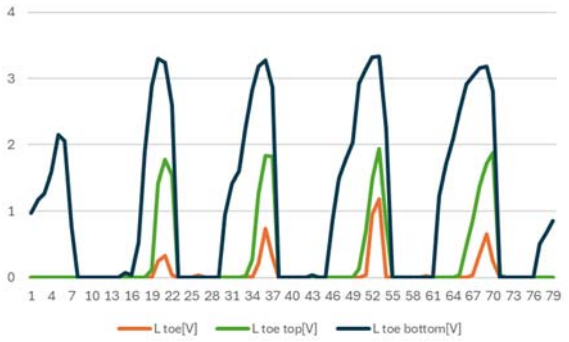

Fig. 11. Left side measurement data after modification (only 3 toe locations).

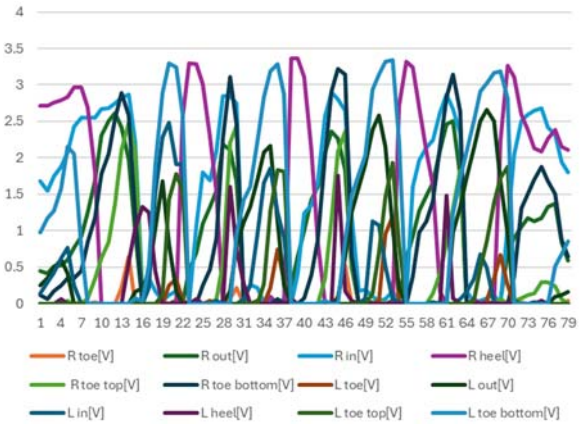

Fig. 12. Measurement data on both sides after modification.

By increasing the number of toe measurement points to three, we were able to confirm that we could measure motion at the tip of the toe (toe-top in the figure), the conventional toe, and the rear end of the toe (toe-bottom in the figure). In addition, the measurement results at the three locations were not the same and measurement results for individual sensor positions could be obtained.

4. Discussion

The collected data were further examined for classification using machine learning. This study employed Random Forest analysis to discriminate between sensors that were expected to have specific characteristics. The data used were the peak values for each sensor extracted from the raw data of the sensor values via from two healthy subjects, and the data based on which the rate of change per hour was calculated for each sensor.

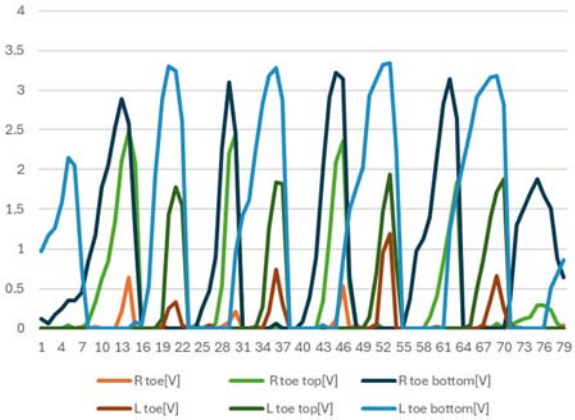

Fig. 13. Measurement data on both sides after modification (only 3 toe locations).

Herein, three measurement conditions were established. (1) normal gait data, (2) gait data with right knee restriction, and (3) gait data with left knee restriction.

The analysis was performed in Python using an analysis program based on Scikit-learn [15], a machine-learning library.

Elements with "-G" in the element names in the figures below indicate the rate of change (rate of change per hour). Elements without "-G" in their element names in the plots indicate the peak value data.

4.1. Analysis by Peak Value and Rate of Change

The peak value and rate of change datasets for Conditions (1), (2), and (3) were analyzed for the two subjects. The results are shown in Fig. 14.

The top eight elements were left heel, left inside-G, left heel-G, right heel, left toe-G, right heel-G, right outside, and right outside-G. There were four heel data points: one inside, one toe, and two outside the heel.

It was confirmed that the order of appearance of the left foot components was high, regardless of the restricted foot. The toes considered important were ranked lower than expected. The reason for the high ranking of the heel data was considered to be that it was a location wherein a greater load was applied compared to the other three locations.

The ratio of peak to rate of change for the top eight elements was 3 for the peak and 5 for the rate of change. Moreover, the ratio of the rate of change was

slightly higher; however, the ratios were almost the same.

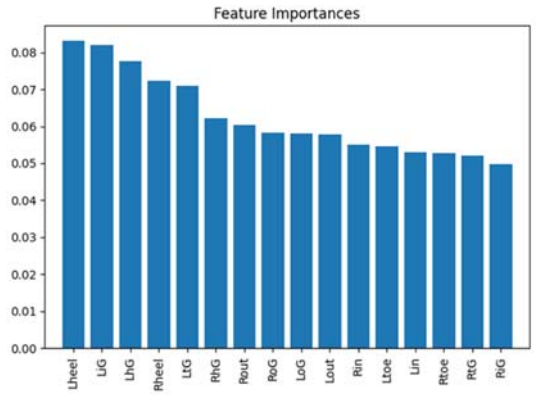

Fig. 14. Results of peak value and rate of change analysis.

4.2. Peak Value Analysis

To examine the existence of a difference between the peak value and rate of change, analyses were performed separately for the rate of change and peak value.

The peak value datasets for conditions (1), (2), and (3) were analyzed. The results of this analysis are shown in Fig. 15. Fig. 15 presents the results of the sensor peak value analysis in the following order of increasing values: left heel, right heel, right outside, left outside, right inside, left inside, right toe, and left toe. The results analyzed based on the peak values exhibited a higher ranking of heel values.

Moreover, a relatively high load on the heel and low load on the toe influenced the order of appearance. This confirmed that a greater load applied to the heel influenced the magnitude of the sensor value.

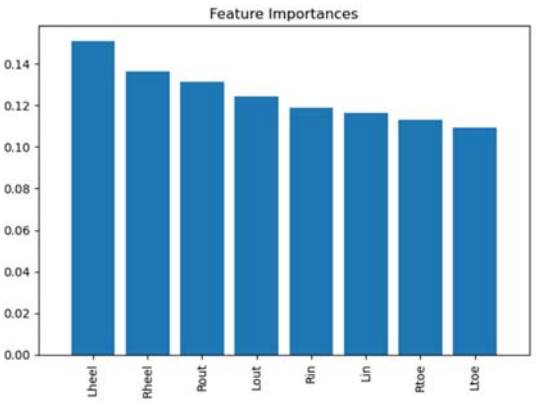

Fig. 15. Analysis results of sensor peak values.

4.3. Analysis by Rate of Change

The rate of change dataset for conditions (1), (2), and (3) was analyzed. The results are presented in Fig. 16.

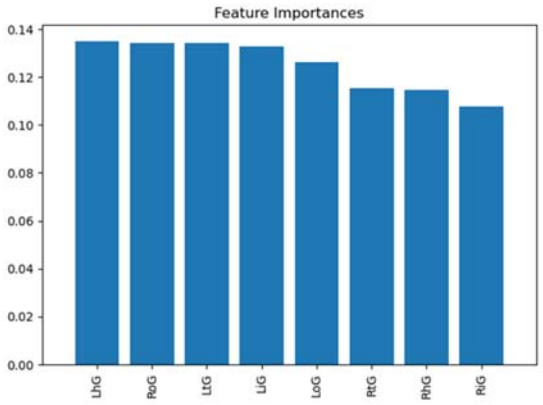

Fig. 16. Result of sensor rate of change analysis.

Fig. 16 shows the results in the order of increasing value: left heel, right outside, left toe, left inside, left outside, right toe, right heel, and right inside. Independent of the restricted foot, the component values of the left heel, Left toe, and Left inside were high. In contrast to the peak value results, the toe component had a higher rank. By examining the rate of change, we determined that the toe data buried in the peak values could be detected.

4.4. Subject Differences Analysis

To confirm the subject differences, the peaks and rates of change of the data for conditions (1), (2), and (3) were analyzed separately for each subject. The results of the data analysis of Subject A (male in his 40s, foot size 27 cm) are shown in Fig. 17. Fig. 17 shows that the four highest values were for the left heel-G, left inside, left inside-G, and left heel. The component value of Left was large, regardless of the restricted foot.

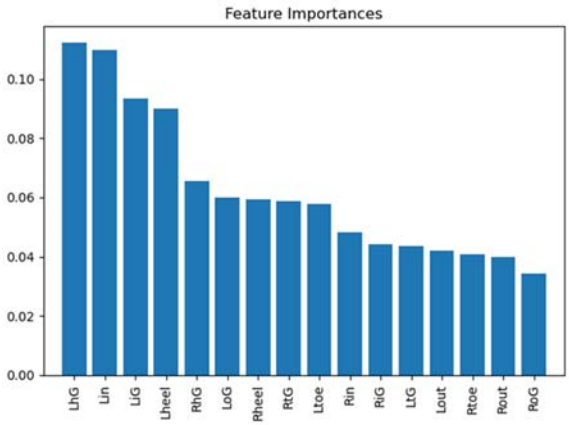

Fig. 17. Analysis results for Subject A.

Fig. 18 shows the results of the data analysis for Subject B (male in his 60 s, foot size 25 cm).

As evident, the top four highest values were for the right outside, left inside, left inside-G, and left toe. The

component values of the left and left toes were large, regardless of the restricted leg.

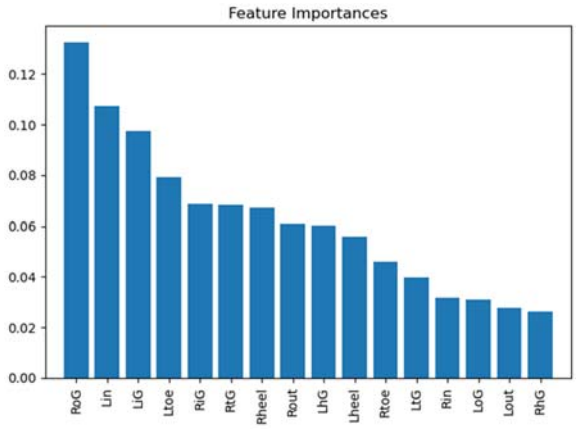

Fig. 18. Analysis results for Subject B.

A comparison of Figs. 17 and 18 revealed that the top four components were different, although the left-side value was high. Further, the composition ratio of the sensor values varied among subjects. In addition, it was possible for each subject to be authenticated according to its frequency of occurrence.

4.5. After Modification

From Section 4.5, the results of the improved toe measurement section will be discussed.

4.5.1. Comparison Using Peak Values at Three Toe Locations after Modification

Peak values were obtained from the data at the three toe locations. Fig. 19 shows the relationship between the sensor position and the average peak value, and Fig. 20 shows the relationship between the sensor position and the maximum peak value. The vertical axis of the graph represents the voltage of the sensor and the sensor position represents the distance from the tip to the center of the sensor, as shown in Fig. 4.

From Figs. 19 and 20, a difference in output was observed at the tip of the toe depending on the limiting condition, with the output value being relatively high. The output value at the rear end of the toe(toe-bottom) was consistently high, but showed minimal variation across different limiting conditions. The central part of the toe showed the largest difference depending on the constraint state; however, the output values obtained were low. Therefore, we considered that data from the tip of the toe, which could not be measured previously, would be more suitable for analysis.

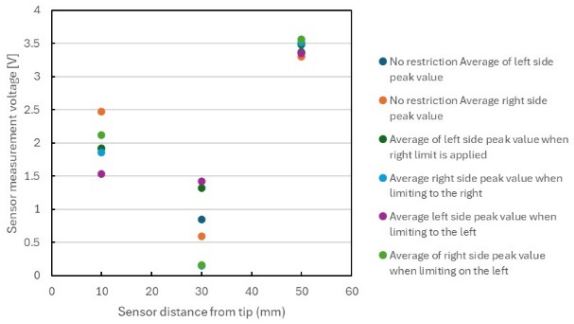

Fig. 19. Relationship between sensor position and average peak value.

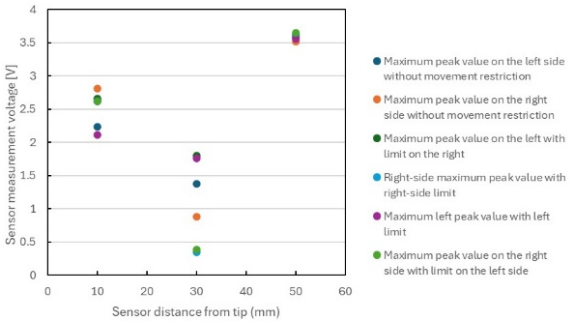

Fig. 20. Relationship between sensor position and maximum peak value.

4.5.2. Examining State Discrimination by Rate of Change of Sensor Values

Figs. 21 through 23 show examples of the rate of change of sensor values obtained at the six locations. Fig. 21 shows an example of a recording of a normal walk. Fig. 22 shows an example recording with the left leg restricted. Fig. 23 shows an example recording with the right leg restricted. This section describes the lines in the figures in Figs. 21-23. The blue line in the illustration indicates the heel, the purple line indicates the top of the toe, the red line indicates the toe, the green line indicates the bottom of the toe, the yellow line indicates the inside of the foot, and the yellow-green line indicates the outside of the foot.

Fig. 21 is compared to Fig. 22 and Fig. 23. In Fig. 22, the left toe bottom (green in the figure) and right toe inside (yellow in the figure) were not synchronized in the unrestricted condition. In Fig. 23, near-synchronous movement between the right toe-bottom and right inside was evident. Although the sample size was is small, we observed a tendency for the toes and insides of the restricted foot to be misaligned in their timing of landing on the ground.

4.5.3. Analysis with Toe Top Data

Using the analysis results of the previous section, the toe data were converted to toe-top data (referred to as toe-top in the figure) and analyzed using a random

forest with the rate of change of the sensor. The results are presented in Fig. 24.

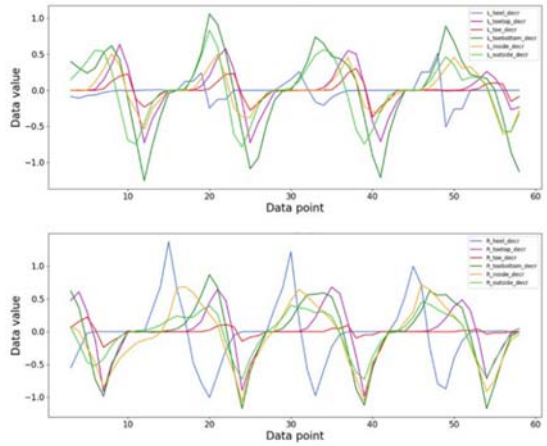

Fig. 21. Percentage change variation of left and right loads for unrestricted measurements (top: left foot, bottom: right foot).

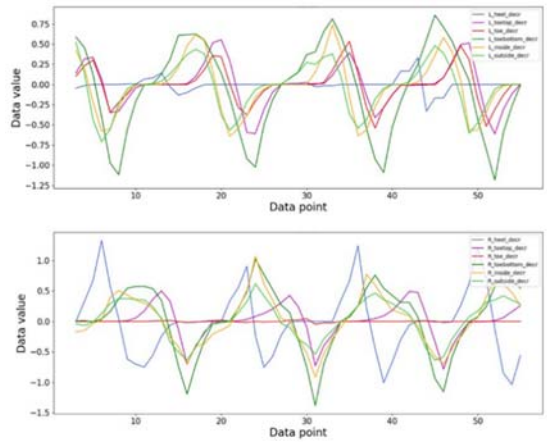

Fig. 22. Variation in rate of change of left and right loads with restriction on the left foot (top: left foot, bottom: right foot).

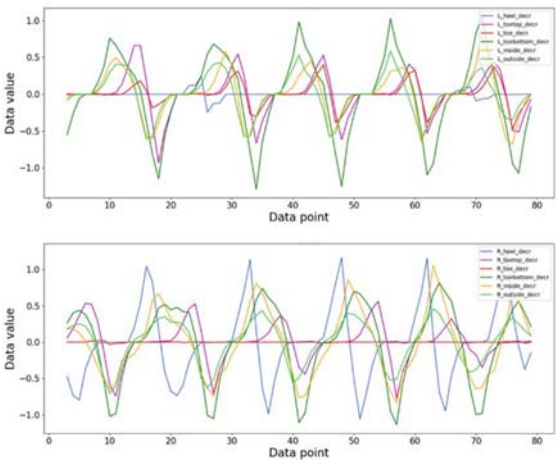

Fig. 23. Variation in rate of change of left and right loads with restriction on the right foot. (top: left foot, bottom: right foot).

Fig. 24 shows the results in order of increasing values: right toe top-G(RttG), left heel-G(LhG), left toe top-G(LttG), right heel-G(RhG), left outside-G(LoG), right inside-G(RiG), right outside-G(RoG), left inside-G(LiG), and right outside-G(RoG), and left inside-G(LiG). Regardless of the restricted foot, the toe and heel component values were high on both feet. The analysis results of the sensor peak values are shown in Fig. 25.

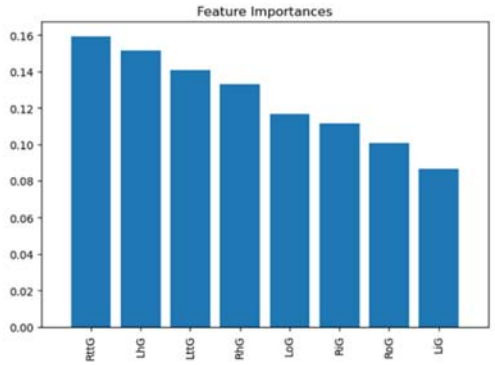

Fig. 24. Results of analysis of sensor change rate.

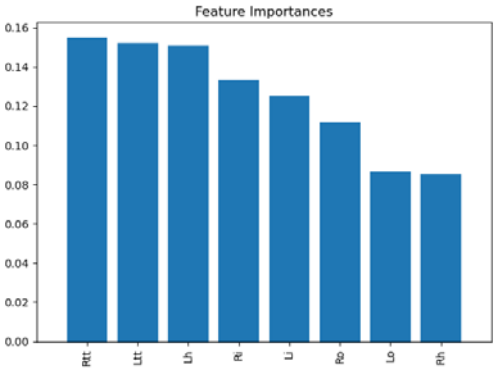

Fig. 25. Analysis results of sensor peak values.

Fig. 25 shows, in order of increasing value, right toe top (Rtt), left toe top (Ltt), left heel (Lh), right inside (Ri), left inside (Li), right outside (Ro), left outside (Lo), right heel (Rh). The top two toe component values for both feet were notably high.

The toe-top component values were judged to be higher than those of the conventional toe from Figs. 29 and 30, suggesting that the toe-top data were useful for discrimination.

4.5.4. Principal Component Analysis by Rate of Change

Principal component analysis was performed based on the results of the random forest analysis described in the previous section. The results of the principal component analysis using sensor change rates are shown in Figs. 26 to 29.

Fig. 26 shows that the first principal component was focused on the right toe (RttG), and the second principal component was focused on the left heel (LhG).

Elements 1-8 are the same as those in Fig. 24. The top four elements in Fig. 27 have cumulative contribution ratios exceeding 0.9, which indicates that the toe and heel factors are significant.

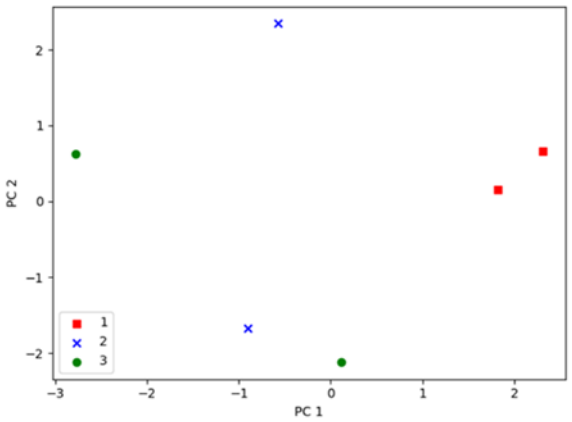

Fig. 26. Contribution of observables using sensor change ratio.

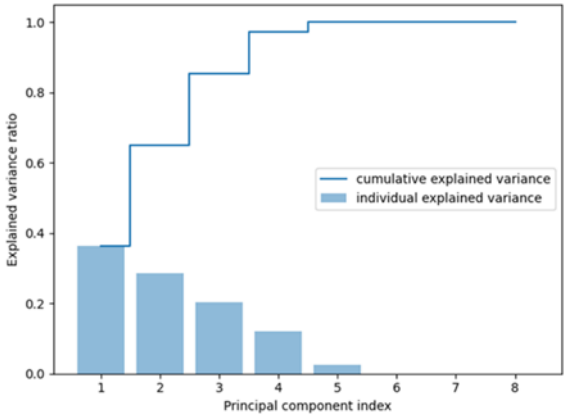

Fig. 27. Contribution and cumulative contribution ratio using sensor rate of change.

Fig. 28 shows the results of the principal component analysis on the supervised data. Although there were some errors, we can see that the three-factor classification was been implemented. Fig. 29 shows the results of classification using the test data. It can be observed that elements 2 and 3 were erroneous, but element 1 was successfully classified.

4.5.5. Principal Component Analysis by Peak Values

Similarly, Figs. 30-33 show the results of the principal component analysis using the peak value data. Elements 1-8 are the same as those shown in Fig. 25.

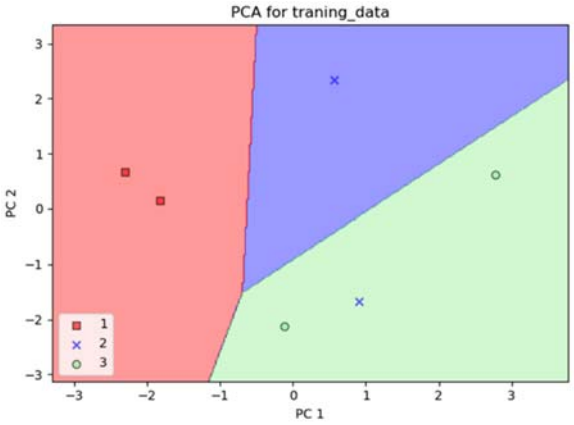

Fig. 28. Classification results using supervised data with sensor change rate.

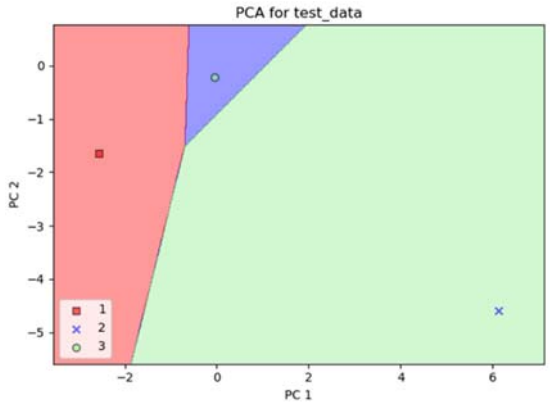

Fig. 29. Classification results based on test data using sensor change rate.

In Fig. 30 shows that the first principal component is focused on the left heel (Lh), and the second principal component is focused on the right toe (Rtt).

Fig. 31, the cumulative contribution ratio exceeds 0.8 for the top three factors, indicating that the toe and heel factors are significant.

Fig. 32 shows the results of the principal component analysis on the supervised data. Although there were some errors, it is evident that the three-factor classification was implemented.

Fig. 33 shows the results of classification using the test data. It can be observed that the classification of the three elements was performed without error.

5. Conclusion

Simultaneous measurement of both feet is now possible using this improved system.

From the acquired data, it is now possible to perform an analysis using features based on the data from both feet. For example, differences in gait state were observed by comparing external measurement data. By obtaining and analyzing the rate of change and peak values from the acquired data, we investigated the possibility of extending the analysis

to machine learning. The results of the analysis using random forest revealed that the toe sensor output was small in this measurement, as shown in the waveform in Fig. 5. We believe that the sensor value has a significant impact on the results of the peak value analysis. It was necessary to investigate whether the toe sensor position was optimal. From the comparison of the data used in the analysis, it appears that the rate of change captures the change during walking, even though the value is small compared to the peak value. This suggests that analysis by the rate of change may lead to the analysis of more detailed information compared to peak values. The results of the first measurement at one location indicated that the toe sensor data might be useful. We then analyzed the data using an insole with additional toe measurement points and demonstrated the possibility of classification by principal component analysis using data from the tip of the toe and between the toes. Although the data presented in this study were from two subjects, the possibility of discriminating between the subjects was found. This finding may lead to an accurate analysis of subject's gait characteristics.

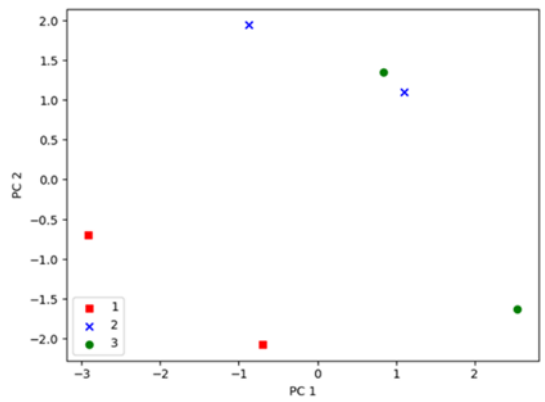

Fig. 30. Contribution of observables using peak values.

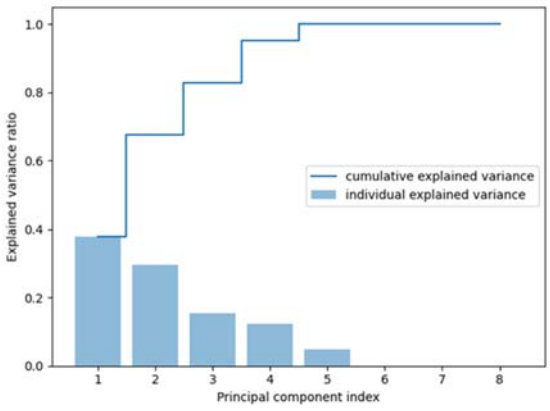

Fig. 31. Contribution ratio and cumulative contribution ratio using peak values.

In this study, we demonstrated the usefulness of insoles that can record detailed toe data tailored to each subject. Further study of the analysis method may enable the classification of the subject's gait condition and provide guidelines for measurement locations according to the subject's symptoms.

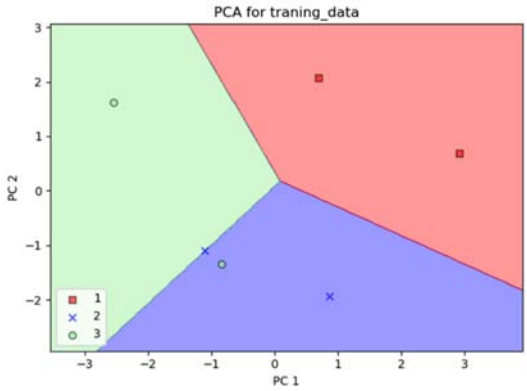

Fig. 32. Classification results with supervised data using peak values.

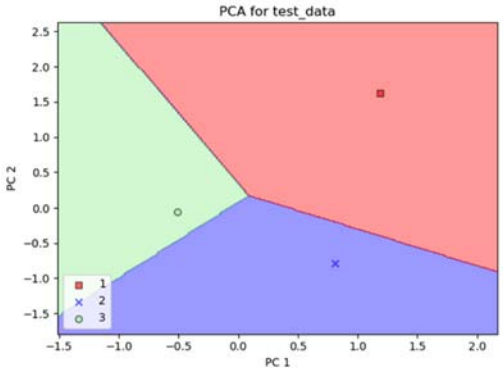

Fig. 33. Classification results from test data using peak values.

Acknowledgements

This study was supported by JSPS KAKENHI, Grant Numbers JP20K11924 and JP23K11207.

References

[1]. T. Kohro, Y. Furui, N. Mitsutake, R. Fujii, H. Morita, S. Oku, K. Ohe, R. Nagai, The Japanese national health screening and intervention program aimed at preventing worsening of the metabolic syndrome, *International Heart Journal*, Vol. 49, Issue 2, 2008, pp. 193-203.

[2]. M. Tago, N. E. Katsuki, S. Yaita, et al., High inter-rater reliability of Japanese bedriddenness ranks and cognitive function scores: a hospital-based prospective observational study, *BMC Geriatr.*, Vol. 21, 2021, 168.

[3]. B. Gunaydin, et.al., Multifractal detrended fluctuation analysis of insole pressure sensor data to diagnose vestibular system disorders, *Biomedical Engineering Letters*, Vol. 13, 2023, pp. 637-448.

[4]. M. Plotnik, N. Giladi, J. M. Hausdorff, Bilateral coordination of walking and freezing of gait in Parkinson's disease, *European Journal of Neuroscience*, Vol. 27, 2008, pp. 1999-2006,
[5]. J. M. Hausdorff, J. D. Schaafsma, Y. Balash, A. L. Bartels, T. Gurevich, N. Giladi, Impaired regulation of stride variability in Parkinson's disease subjects with freezing of gait, *Experimental Brain Research*, Vol. 149, 2003, pp. 187-194.
[6]. 3D motion capture system "VICON", https://www.vicon.com/
[7]. Tekscan Pressure Sensitive Mats, https://www.tekscan.com/versatile-pressure-sensing-mats
[8]. A. Kammoun, P. Ravier, O. Buttelli, Comparison of the accuracy of ground reaction force component estimation between supervised machine learning and deep learning methods using pressure insoles, *Sensors*, Vol. 24, Issue 16, 2024, 5318.
[9]. Toyoda Gosei, Feelsole, https://www.toyodagosei-led.jp/en/feelsole/
[10]. Moticon OpenGO, https://moticon.com/opengo/sensor-insole-sizes
[11]. Y. Uchida, T. Funayama, E. Ohkubo, Y. Kogure, Feature value classification based on the position difference of pressure sensors installed in insoles and their outputs, *Sensors & Transducers*, Vol. 263, Issue 4, 2023, pp. 12-20.
[12]. T. Funayama, Y. Uchida, Y. Kogure, D. Souma, R. Kimura, Exploring the assessment of steps using insoles with four-part pressure sensors, *Sensors & Transducers*, Vol. 263, Issue 4, 2023, pp. 21-28.
[13]. E. Ohkubo, Y. Uchida, T. Funayama, Y. Kogure, Prototype of bilateral gait measurement system and its initial analysis, in *Proceedings of the 10th International Conference on Sensors and Electronic Instrumentation Advances (SEIA'2024)*, Spain, 25-27 September 2024, pp. 39-43.
[14]. Interlink FSR-402, https://www.interlinkelectronics.com/fsr-402
[15]. Scikit-learn Project, https://scikit-learn.org/stable/

Published by International Frequency Sensor Association (IFSA) Publishing, S. L., 2024 (http://www.sensorsportal.com).